

We are IntechOpen, the world's leading publisher of Open Access books Built by scientists, for scientists

4,800

Open access books available

122,000

International authors and editors

135M

Downloads

Our authors are among the

154

Countries delivered to

TOP 1%

most cited scientists

12.2%

Contributors from top 500 universities



WEB OF SCIENCE™

Selection of our books indexed in the Book Citation Index
in Web of Science™ Core Collection (BKCI)

Interested in publishing with us?
Contact book.department@intechopen.com

Numbers displayed above are based on latest data collected.
For more information visit www.intechopen.com



Intelligent Laparoscopic Assistant Robot through Surgery Task Model: How to Give Intelligence to Medical Robots

Dong-Soo Kwon, Seong-Young Ko and Jonathan Kim
*Korea Advanced Institute of Science and Technology
Republic of Korea*

1. Introduction

Laparoscopy has become one of the most popular surgical techniques since the 1990s due to its surgical effectiveness, fast recovery and good cosmetic outcome. From simple to more complex surgeries, the proportion of laparoscopic to open procedures is continuously increasing. Due to small incision, patients can regain health without much trauma and hospitalization; however, the operating surgeons suffer from limited range of motion, reduced flexibility, loss of tactile sensation and limited depth perception compared to open surgery. One of the important issues for successful surgery is the cooperation between the operating surgeon and the assistant as it is directly related to how the surgeon can perform surgical tasks. Manipulating vessels and organs using long tools without direct visual feedback requires utmost attention and the assistant should maneuver the laparoscope without disrupting the operating surgeon. Novice assistants often suffer from: (a) the difficulty in properly positioning the laparoscope in three-dimensional space based on the projected images on a monitor, (b) the presence of the fulcrum effect at the trocar insertion point, and (c) the hand tremor caused by fatigue. To alleviate the effect of these difficulties, some surgical robotic systems (Franzino, 2003; Ghodoussi et al., 2002; Guthart & Salisbury, 2000; Mitsuishi et al., 2003) and laparoscopic assistant robot systems such as AESOP (Wang et al., 1996), EndoAssist (Finlay, 1996) and so forth (Berkelman et al., 2002; Kobayashi et al., 1999; Taylor et al., 1995) were developed.

Despite the applicability in real surgeries, these systems exhibit some common limitations or constraints that should be resolved. These systems are known to occupy a voluminous space in the operating room and the external motion of links tends to interfere or come in close contact with the surgeon and surgical staff. In order to develop a compact robot and to reduce possible interference with surgical staff, we adopted an internally bending mechanism. This internally bending mechanism confines the majority of motions inside the patient's abdomen and also reduces the size of the robotic system. The proposed laparoscopic assistant robot system, KaLAR (KAIST Laparoscopic Assistant Robot), will be explained in detail later.

Although most of the robotic assistants can substitute for the role of human assistant, clinical studies revealed that a considerable number of voice commands are needed to control the robot, while only a handful of voice commands is sufficient with a human

Source: Medical Robotics, Book edited by Vanja Bozovic, ISBN 978-3-902613-18-9, pp.526, I-Tech Education and Publishing, Vienna, Austria

assistant. Another modality of control such as the use of surgeon's head motion can be used, but this does not completely eliminate the need for voice commands and may introduce additional physical stress (Nishikawa et al., 2001). Surgery requires delicate handling of tissues at the surgical site and the burden of controlling the robot should be kept minimal. Since lesser control burden is imposed on the operating surgeon when aided by a human assistant, a skillful human assistant is a good example of how a robotic assistant should behave. A key difference between a human assistant and a robotic assistant lies in the degree of preliminary knowledge of the surgery. Therefore, in order for the robot to become an intelligent assistant rather than a motorized surgical tool, it should have preliminary surgical knowledge similar to a well-trained human assistant. The ideal method may be to develop a complete human-like robot with both human-level artificial intelligence and interaction capability; however, considering the state-of-the-art in current robotic technology, this remains a distant goal. Although achieving a general surgical intelligence may be difficult, it is possible to achieve *task-specific* intelligence for laparoscopic assistant robot through a surgery task model, considering its specific task domain and restrictive behavior patterns.

The remains of this chapter will present the laparoscopic assistant robot system and the interaction method based on a surgery task model. In section 2, the details of the robot system will be explained. Section 3 will describe the concept and implementation of the interaction method based on a surgery task model. Section 4 will demonstrate the preliminary result of the proposed robotic system and the interaction scheme based on a surgery task model. Finally, conclusions and discussions for future work are presented in section 5.

2. Compact Assistant Robot for Adjusting Laparoscope View

2.1 Basic Concepts and Workspace Requirements

In this section, our compact laparoscopic assistant robot, KaLAR, will be explained (Kim et al., 2004; Lee, 2004). KaLAR makes the use of a bending mechanism that is composed of several articulated joints. The robotic system can generate 3-DOF motion, including 2-DOF internal bending motion and 1-DOF external linear motion. Until now, various bending mechanisms have been developed for application in laparoscopic surgery (Ikuta et al., 2003; Simaan et al., 2004; Yamashita et al., 2003). These mechanisms were mainly focused on improving the mechanical characteristics of the bending mechanism for performing surgical manipulation rather than controlling a laparoscope. Although our system does not require high accuracy in position control, it requires relatively wide area of open space for electronic wires for CCD module, mechanical wires for articulated joints and optical fiber bundle for light source and therefore, a much simpler bending mechanism consisting of many thin, hollow cylindrical links (Tanaka, 1978) was adopted.

To determine the range of viewing angle in conventional laparoscopy, we made observations during human cholecystectomies. Cholecystectomy is the surgical removal of the inflamed or stoned gallbladder and is the most common procedure for laparoscopy. In general, 4-DOF motion is available in conventional laparoscopic surgery (Çavuşoğlu et al., 2001). There are mainly two rotations (up/down and left/right) about two axes on the incision surface, a translation (in/out) along the axis perpendicular to the incision surface,

and an axial rotation. Since the axial rotation is not fully utilized, we have not implemented this feature in our system.

Our observation shows that the ranges of up/down and left/right movements are within 30 degrees while the range of in/out movement is approximately 100mm during normal operation, as shown in figure 1. The range of this in/out motion is in accordance with the result reported by Riener et al. using an electromagnetic position sensor (Riener et al., 2003). Based on this observation of the necessary workspace, we have developed a laparoscopic assistant robot that can cover the full range of view required for human cholecystectomy.

2.2 Design of Compact Laparoscopic Assistant Robot

The overall design of the developed robot is as shown in figure 2. The direction of views can be altered by changing the alignment of the articulated joints while magnification/reduction of view can be altered by moving closer or away from the surgical site using a linear actuator. Since KaLAR itself functions as a laparoscope, a CCD camera module and a bundle of optical fibers are installed at the tip of the bending section as shown in figure 2 and they are directly connected to the image capturing unit and a xenon light source.

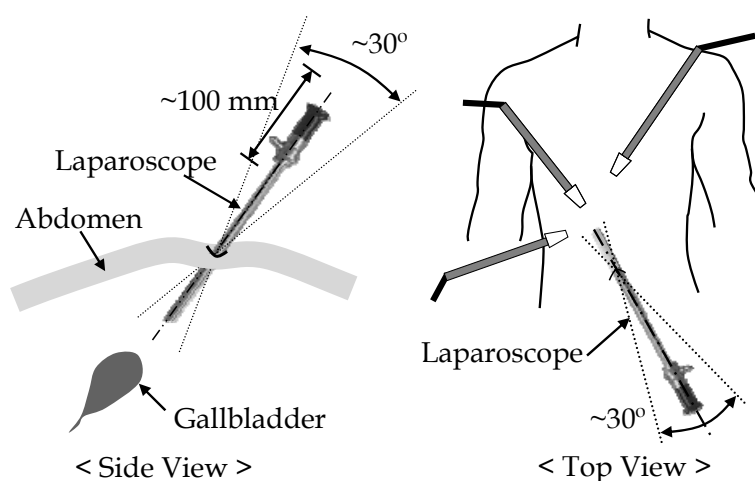


Figure 1. Range of motions in human cholecystectomy

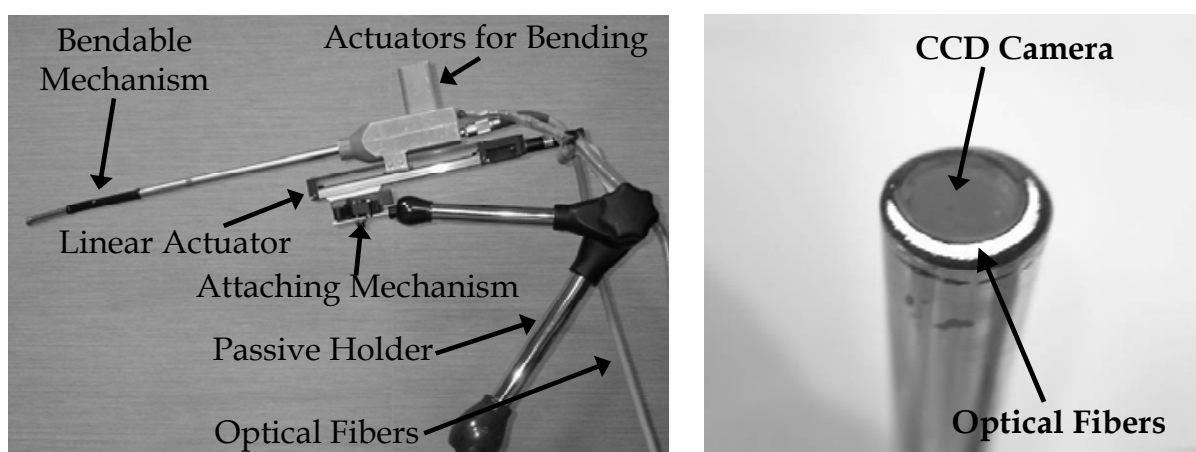


Figure 2. The developed compact laparoscopic assistant robot

2.2.1 Bending Motion

The bending mechanism consists of a series of thin, hollow cylindrical links connected by small joints and each link has two or four guiding holes inside as shown in figure 3. For internal bending motion, the most distal link is connected to two wheels through two pairs of steel wires, which are guided by guiding holes in the joints. There are 2 guiding holes inside each link except two links on both ends of the bending mechanism. The two links on both ends have 4 guiding holes and the wires passing through the guiding holes are distally connected to the CCD module and proximally to two wheels. The two wheels of different sizes are directly attached to corresponding motors as shown in figure 4. For controlling the bending mechanism, rotation of the motor changes the tension in the wires and thus, changes the orientation of each joint as shown in figure 5. For safety and initialization, two stoppers and photo sensors are placed to fix the bending range as shown in figure 4.

We have determined the range of motions of a rigid laparoscope in section 2.1 and comparable range of motion must be possible with the bending mechanism. To determine how much of bending is required for comparable viewing range, we have simulated the motion using approximated parameters in laparoscopy and design constraints. For installation of a CCD module and a bundle of optical fibers at the tip, approximately 70 mm of length is required. From the observation, the distance between the navel and the gallbladder is approximately 200 mm and in some cases, laparoscope may be placed 30~50 mm apart from the gallbladder during surgery. The bending section is 23 mm long and it is composed of 7 circular links connected by 6 joints. In conjunction with an assumption that bending of links will form a circular shape with a constant radius, we can compute the

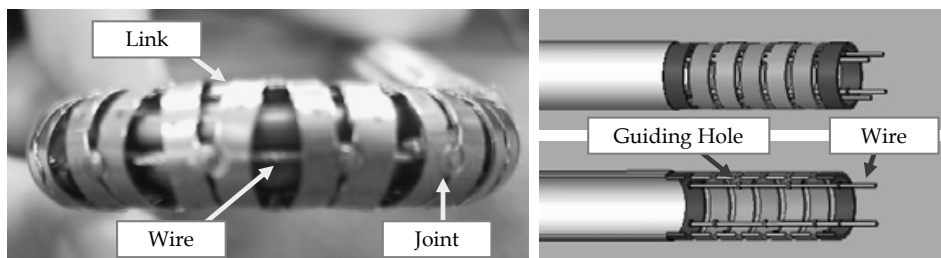


Figure 3. Wire-driven bending mechanism

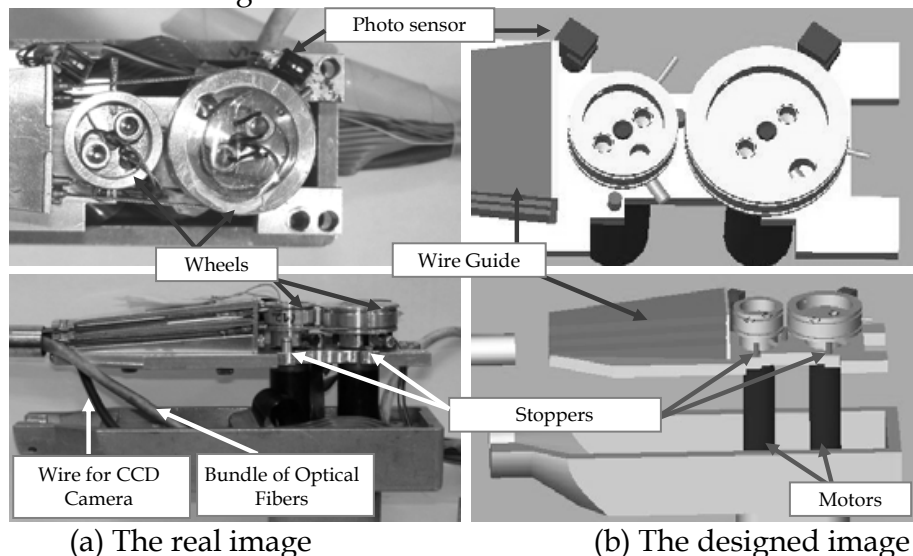


Figure 4. Configuration of wheels and motors for bending motion

required bending angle for comparable viewing range. As shown in figure 6, about 30 degrees of bending angle will have the equivalent viewing angle as a rigid laparoscope rotates 15 degrees about the insertion point. If the robot is positioned farther than 30 mm from the region of interest, the viewable range will be greater than that of a rigid laparoscope. For making the installation procedure more flexible, we've configured two limit sensors so that bending can take place from -60 to +60 degrees in each direction.

2.2.2. In/Out Motion and Sterilization

For moving closer and away from the surgical site, a linear actuator consisting of a linear motion guide, a ball screw, and a brushed DC motor was installed. In order to cover the necessary workspace, we chose the linear actuator with 130mm stroke length. This linear actuator is connected to a passive laparoscope holder by a connector similar to the one used to join a camera and a tripod as shown in figure 7. The use of this passive holder allows the surgeon to readily install the robot to the bedside.

To sterilize the KaLAR system, moving portion of the robot, which includes the upper part and the linear actuator, is made separable from the passive holder unit and thus, both the robot and the passive holder can be easily sterilized with ethylene oxide gas.

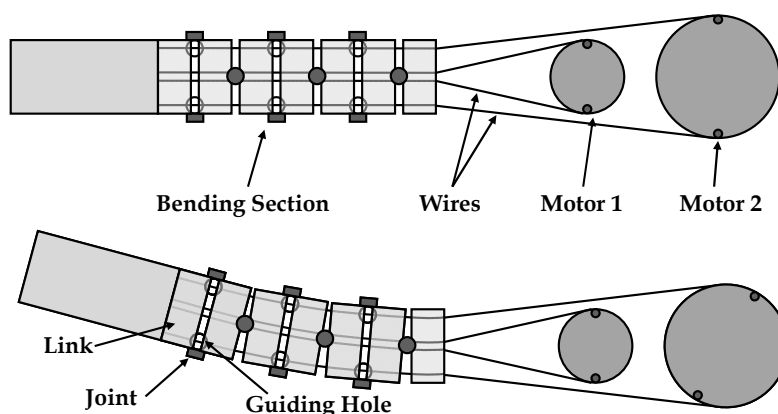


Figure 5. Wire-driven bending mechanism with motors

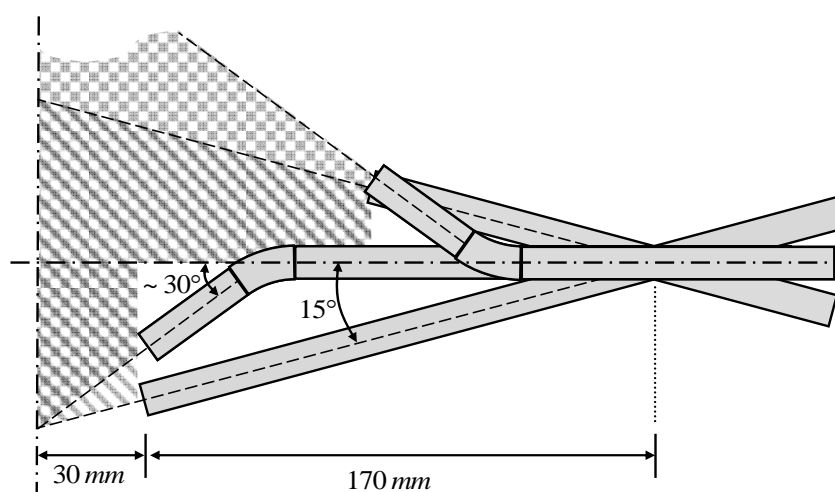


Figure 6. Workspace comparison between a rigid scope and the proposed system

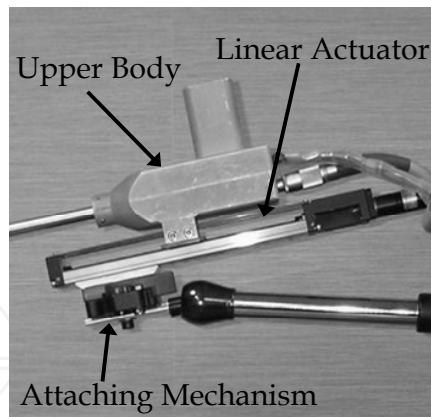


Figure 7. 2-DOF upper body and linear actuator connected to a passive laparoscope holder using attaching mechanism

2.3 Hysteresis Compensation in Bending Mechanism

Interesting characteristics of the bending mechanism are the linearity and hysteresis. Ideal mathematical modeling of the bending mechanism shows that its bending angle ($\theta_{up/down}$, $\theta_{left/right}$) moves highly linear relative to wire length variation ($\Delta l_{w_{up/down}}$, $\Delta l_{w_{left/right}}$) (Ko et al., 2007a). However, since the real bending mechanism has a play in joints and guiding holes, the behavior of the bending mechanism has considerable hysteresis. Figure 8 shows the block diagram of a low-level control structure including the hysteresis compensation. The compensation is conducted by adding the measured average offset value to the desired input only if the input is increasing. This compensation scheme can be expressed by (1). In case of the linear (zoom-in/-out) motion, no compensation is made due to no observed hysteresis effect.

$$\Theta_{comp,i} = \Theta_{hys,i} \times \frac{\text{sign}(\dot{\theta}_{des}) + 1}{2} \quad (1)$$

where $\Theta_{comp,i}$ indicates the value of hysteresis compensation of each motor, $\Theta_{hys,i}$ indicates the value of measured hysteresis and $\dot{\theta}_{des}$ indicates the velocity of the desired input.

This simple hysteresis compensation scheme may produce a discontinuity in the desired value. Since the discontinuity causes an abrupt and unstable transition between views,

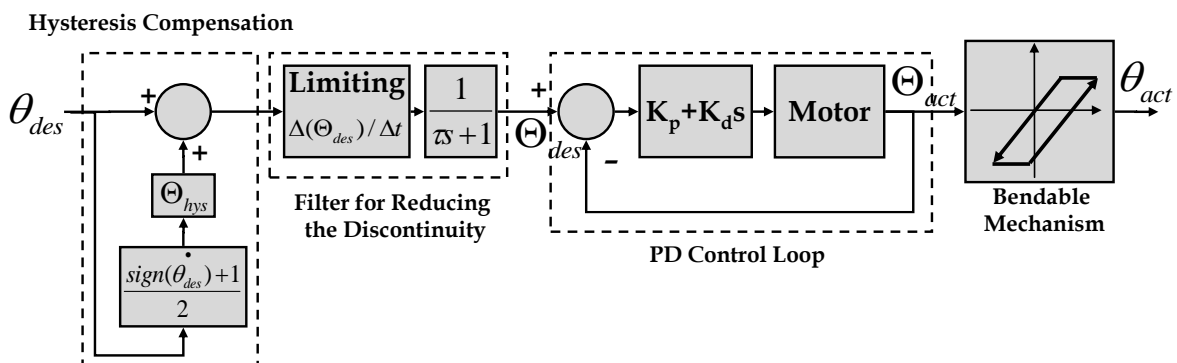


Figure 8. Block diagram of low-level control system

maximum deviation of the desired value is limited to a predefined maximum speed ($\dot{\theta}_{\max}$). We've determined these values to be roughly 11.2°/sec for bending motion and 8mm/sec for linear motion. This method can be expressed by (2) to (4).

$$\Delta_d(k) = \theta_{des}(k) + \Theta_{comp}(k) - \Theta_{beforeLPF}(k-1) \quad (2)$$

$$\text{if } (|\Delta_d(k)| > \dot{\theta}_{\max} \times \Delta T)$$

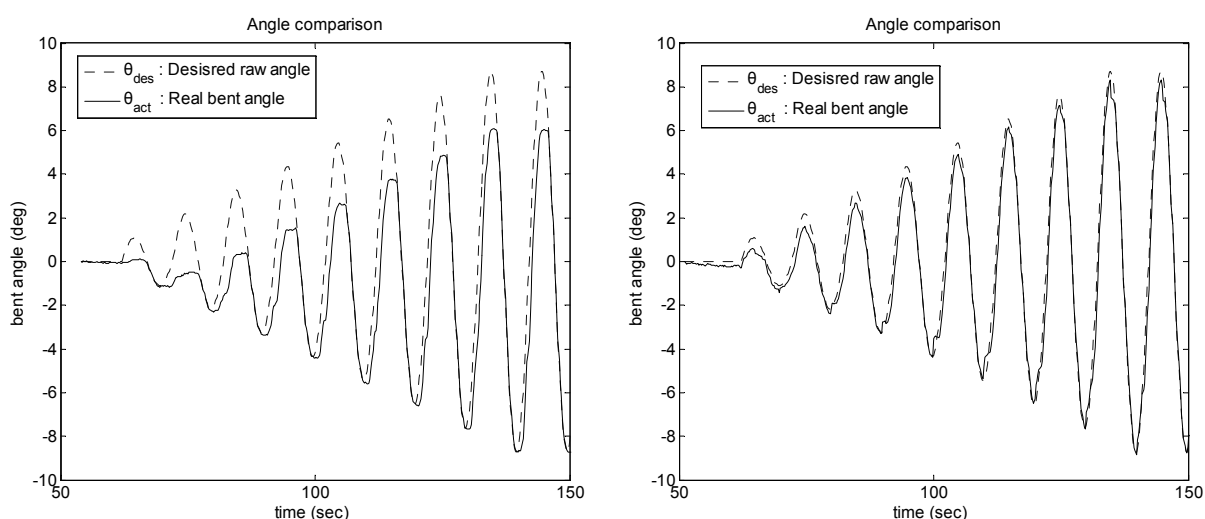
$$\Theta_{beforeLPF}(k) = \Theta_{beforeLPF}(k-1) + \dot{\theta}_{\max} \times \Delta T \times \text{sign}(\Delta_d(k)) \quad (3)$$

else

$$\Theta_{beforeLPF}(k) = \theta_{des}(k) + \Theta_{comp}(k) \quad (4)$$

where $\Theta_{beforeLPF}$ indicates the desired position value, Θ_{comp} indicates the value calculated by (1), θ_{des} indicates the desired input and ΔT is the sampling time.

The $\Theta_{beforeLPF}$ obtained by equation (3) or (4) goes through a first order low pass filter with $\tau=0.03$ sec for eliminating the discontinuity in velocity and the result value is regarded as the final desired input Θ_{des} for a PD controller. As shown in figure 8, the low-level controller does not form a perfect closed loop but it is sufficiently controllable under the assumptions that there is no external force acting on the moving tip and that the surgeon can see the laparoscopic view on the monitor. Figures 9(a) and 9(b) show the tracking performance during the left/right swing motion before and after the hysteresis compensation.



(a) Without hysteresis compensation

(b) With hysteresis compensation

(error_{max} = 3.86°, error_{min} = -0.38°, error_{std} = 1.36°) (error_{max} = 1.76°, error_{min} = 0.0°, error_{std} = 0.51°)

Figure 9. Tracking performance without and with hysteresis compensation

2.4 High Level Control Method : A User Interface

This section explains a higher-level control method of the KaLAR system, which is related to the generation of the desired position (θ_{des}) from the surgeon's command. We adopted both a voice interface and a visual-servoing method to control the system. Voice recognition is implemented based on a speaker-independent software module and thus, requires no

training. Since voice interface is one of the most intuitive control methods, it is used in many laparoscopic assistant systems (Allaf et al., 1998), but it has a limitation of requiring many voice inputs in case continuous view changes are required. To overcome this shortcoming, a visual-servoing method (Casals et al., 1996; Nishikawa et al., 2003; Wang et al., 1996; Wei et al., 1997) was developed. But the sole use of visual-servoing is not sufficient for the complete control of the robotic system. Therefore, we've combined the voice interface and the visual-servoing. The operating surgeon can choose between the voice interface and visual-servoing using a voice command. It can be also determined automatically based on the surgery task model, which will be explained in section 3 in detail.

2.4.1 Voice Interface

As shown in figure 10, voice commands are used to determine the robot's state and the control mode. After an initialization process, the system is in the *pausing state* and waits for the surgeon's command. Upon "start" command by the surgeon, the robot system is placed in the *controlling state* where the robot can be physically activated for specific movement and image processing. To pull the robot out of the *controlling state*, "pause" command is required. In the *controlling state*, the surgeon can choose the control mode using voice commands "tracking mode" or "voice mode." In the *voice command mode*, the surgeon manipulates the surgical view using the commands "go up," "go down," "go left," "go right," "zoom in," and "zoom out." These commands move the robot toward the corresponding direction by predetermined amounts, about 4 degrees per command for bending and 20 mm per command for a linear motion. The *auto-tracking mode* is for tracking the primary surgical instrument marked with color markers. In this mode, 2-DOF bending motion is controlled by visual-servoing while the in and out motion with respect to the abdomen is still controlled by the voice commands "zoom in" and "zoom out." For additional convenience, 2-position memory function is also implemented using the commands "remember position 1," and "remember position 2," and the stored positions can be retrieved by the commands "go to position 1" and "go to position 2."

2.4.2 Visual-Servoing

Visual-servoing is expected to alleviate the surgeon from issuing a great number of voice commands in times of frequent change of camera views. The visual-servoing algorithm is based on the result of other researchers (Casals et al., 1996; Nishikawa et al., 2003; Wang et al., 1996; Wei et al., 1997). Unlike the previous works, a color marker composed of two-color band is placed at the tip to locate the tip of the instrument in the captured image and to identify the tool's type as shown in figure 11 (Ko et al., 2007a). The two-color band is composed of three parts: *near*(P_1), *middle*(P_2) and *far*(P_3) part, named by the distance from the tip. The near and the far parts from the tip are marked with bright cyan for it is rarely found in the internal organs (Wei et al., 1997). These parts have different thickness and are used to locate the direction and position of the tool tip. Since the real distances (D_{1t} and D_{12}) between markers and the tip in figure 11(b) are known, we can obtain the tip position with a simple equation (5), in which the effect of a perspective view is neglected for the sake of simplification. The color of the middle part is used for identifying the type of the tool that is inserted and thus, is utilized to verify the marker detection and to upload the geometric information of the tool.

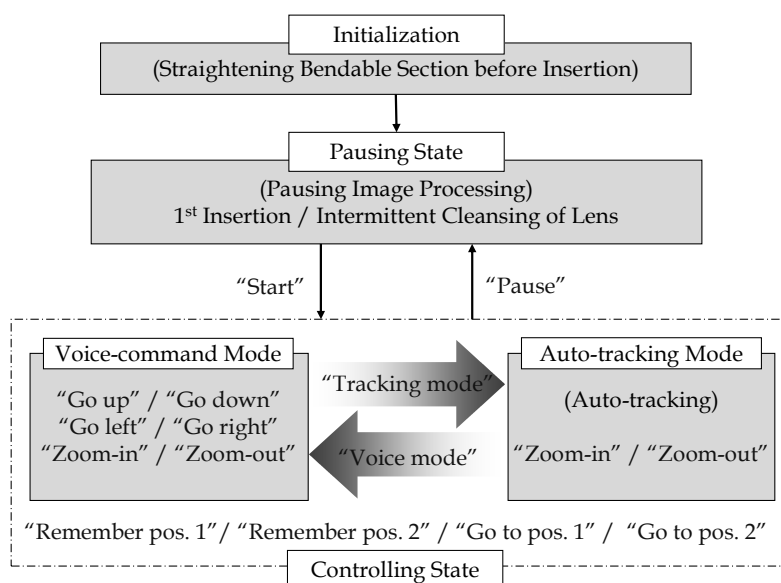


Figure 10. Robot's states and available voice commands

$$P_t = P_1 + |P_2 - P_1| \frac{D_{1t}}{D_{12}} \frac{P_1 - P_3}{|P_1 - P_3|} \quad (5)$$

To avoid the surgeon's motion sickness, visual-servoing is activated only when the tip is moved out of the small portion at the center of a monitor screen. The size of the portion and the maximum bending speed during *in vivo* porcine cholecystectomies were determined by the operating surgeons' preference before the surgery began and were approximately 11.2deg/sec and 30% of the monitor screen, respectively.

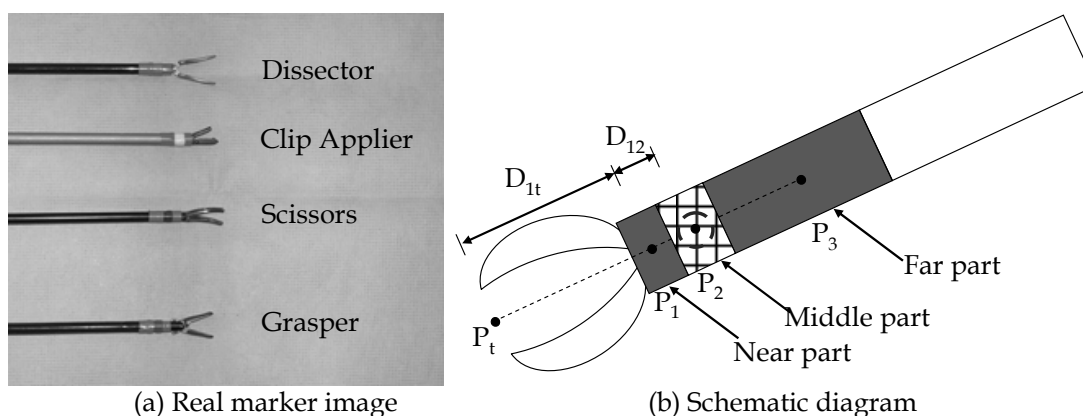


Figure 11. Color markers on surgical instruments

2.5 Overall System Configuration

The main controller is based on a Pentium 4 2.8GHz PC running under Windows 2000. Model 626 board from Sensoray Co. Inc. is utilized for performing low-level position control and for generating hardware interrupts. VoiceEZ software from Voiceware Co. Ltd. is utilized for recognizing the surgeon's voice commands and for synthesizing voice instructions. For convenience, a wireless headset from Inter-M Co. Ltd. is used. Matrox Meteor-II frame grabber board from Matrox Co. and a small CCD camera (IK-M43S) from

Toshiba Co. are used for image processing. In the developed software module, three threads were implemented, each accounting for position control, voice recognition and image process. Sampling in the PD controller is conducted at 1000Hz and image processing is done at the minimum rate of 25 Hz. Since the CCD camera module can support multiple outputs, the laparoscopic view is delivered simultaneously to the image grabber and a super VHS recorder, which is connected to a high definition monitor, as shown in figure 12.

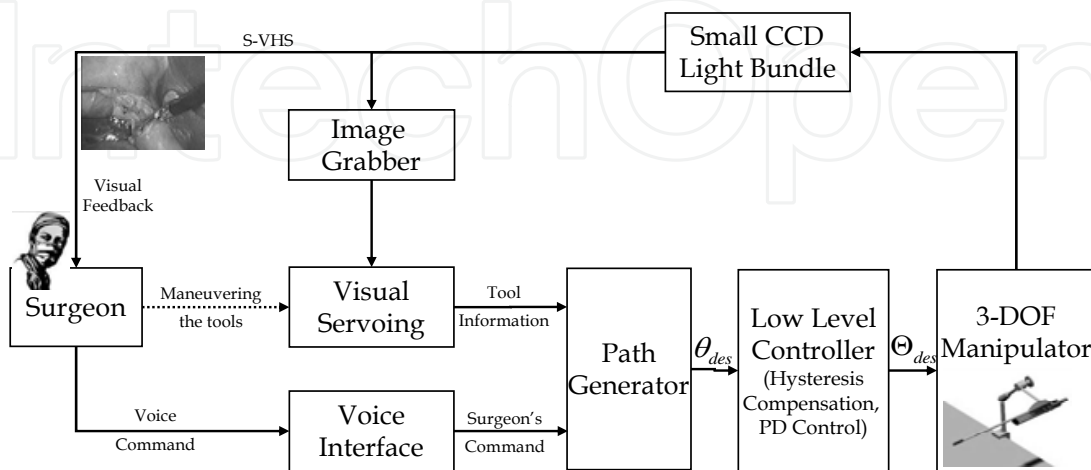


Figure 12. Overall system configuration

3. Surgery Task Model based Interaction

3.1 A Basic Concepts and Backgrounds

As mentioned in Introduction, we believe that an intelligent assistant robot should have the preliminary surgical knowledge similar to that of a well-trained human assistant. A structured preliminary surgical knowledge is defined as a *surgery task model*. Based on this premise, figure 13 illustrates the basic concept of our interaction scheme based on a surgery task model. Unlike other previous assistant robot systems that only follow a surgeon's direct commands, the robot system having the surgery task model responds to surgeon's behavior and performs predefined tasks. This concept can be considered as a specific form of a general human-robot interaction (HRI) structure proposed for an ultimate service robot system with relatively high cognition (Lee et al., 2005; Yoon, 2005). The proposed structure insisted that the HRI should include a task model, a user model, a mental model, a needs model and an interaction model. In case of surgical assistant robot, whose work domain is relatively specific and has restrictive behavior, the interaction scheme with only a task model is sufficient to be applied to a laparoscopic assistant robot. This assistant robot with a surgery task model can acquire information of the surgical environment, estimate current surgical task based on the task model, and finally can suggest appropriate actions, such as maneuvering of a laparoscope.

Some methods for task analysis and task modeling have been developed. In efforts to analyze tasks efficiently, Goals, Operators, Methods and Selection (GOMS), Task Action Grammar (TAG), and so forth have been studied by human-computer interaction research groups (Johnson, 1992). In order to describe a discrete event system, modeling methods based on state-transition models such as automata, Petri-net, and etc. have been studied (Cassandras & Lafortune, 1999). Recently, these task analysis methodologies have been applied

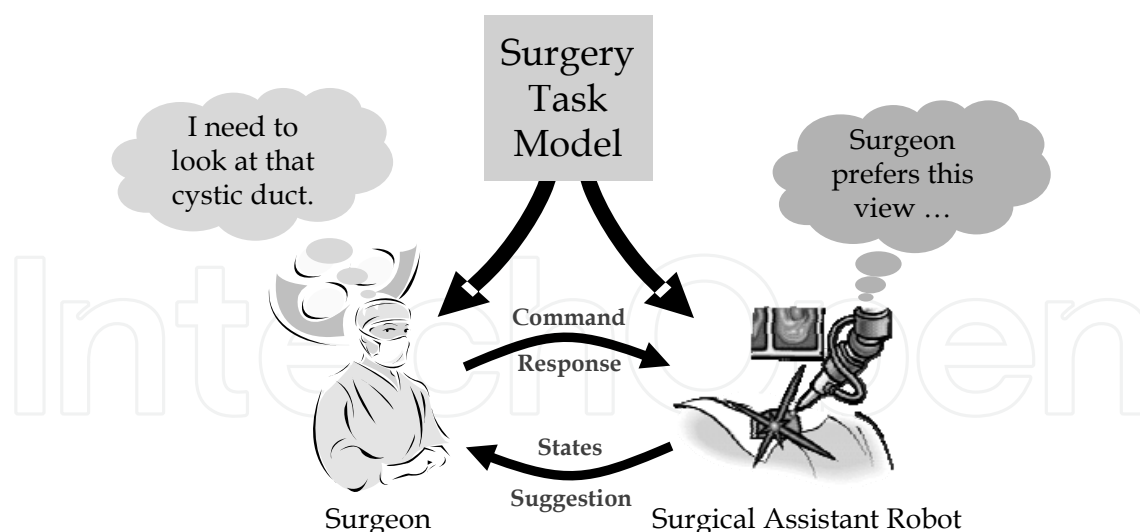


Figure 13. Basic concept of the interaction between a surgeon and a surgical assistant robot

to medical and medical robotics fields. MacKenzie and his colleagues constructed a hierarchical decomposition of Nissen fundoplication, a type of laparoscopic surgery for stopping the reflux of stomach acid, based on a hierarchical task analysis (HTA) (MacKenzie et al., 2001). The procedure was broken down into a sequence of surgical steps and these steps were further broken down into surgical sub-steps, tasks, sub-tasks, and finally primitive motions. Their work showed that a surgical procedure can be expressed with a sequence of decomposed surgical steps, and this decomposition provides a method to evaluate the effectiveness of a surgical procedure, including the procedure with new surgical techniques or new tools. However, this model did not consider the variance in surgery and the role of the surgical robot. Ohnuma and his colleagues suggested a model for an operating scenario based on timed automata including a surgical task, a surgeon, a scrub nurse or a scrub nurse robot, a patient, and their interaction (Ohnuma et al., 2005). This model was integrated into a scrub nurse robot for control. However, it deals with a simplified surgical procedure and the associated analysis is not applicable for controlling a laparoscope. Rosen et al. proposed a modeling method for minimally invasive surgery using a discrete Markov model for assessing surgical performance (Rosen et al., 2006). Their modeling method is a bottom-up approach; they constructed a discrete Markov model from a sequence of tool motions, which are defined by the position and orientation of the tool and the exerted force and torque. Their modeling approach provides a generalized method for decomposing a surgical task. However, it can only assess surgical performance and thus, cannot be applied to surgeon-robot interaction.

In this section, a surgery task model, which can cope with variance in the surgical procedures, is proposed for a laparoscopic assistant robot.

3.2 Definition of Surgery Task Model

A *surgery task model* is defined as a structured form of surgical knowledge that is necessary for a surgeon to perform a specific surgery, including *surgical procedures*, *input information* for identifying the current surgical states, and *action strategies* at each surgical state (Ko et al., 2007b). While it would be an onerous task to standardize or quantify each step of surgery,

simple surgical procedures such as a cholecystectomy can be decomposed into discrete steps.

To allow the task model to include the variance in surgery, state-transition modeling method is utilized. States are defined as sub-procedures, i.e. *surgical stages*. Transitions are defined as changes among surgical stages. The transitions are triggered when the *input information* of the external environment satisfies the predefined conditions. Each surgical stage has a specific *action strategy*. Considering that the model will be applied to a laparoscopic assistant robot, the surgical view captured by a laparoscope and the surgeon's commands were determined as the input information. The type of tool is identified from the surgical view and utilized to trigger transitions between the surgical stages, and the tool position and the surgeon's voice commands are utilized to determine the surgical view based on predefined action strategies.

3.3 Surgical Procedure

As a first step, 8 cases of human-assisted human cholecystectomy were recorded and analyzed in terms of laparoscopic view and operating room view. Using both views, each surgical procedure was decomposed into meaningful surgical stages based on their goal and primary surgical tools in use as shown in Table 1.

No. of Surgical Stages	The Primary Goal	The Primary Surgical Tools/Devices
0	Start	Forceps & Trocar for Lap.
1	Preparing Laparoscope	Positioning a Laparoscope
2	Inserting Trocar for Right Hand and Examining Briefly	Forceps & Scalpels & Trocar
3	Inserting Trocars for Left Hand	Forceps & Scalpels & Trocar
4	Lifting Liver	Ratchet Grasper / Dissector
5	Exposing Artery/Duct	Dissector
6	Clipping Artery/Duct	Clip Applier
7	Cutting Artery/Duct	Scissors
8	Separating Gallbladder(GB) with Dissector	Dissector
9	Separating GB with Cautery	Cautery
10	Inserting Pouch	Extracting Laparoscope & Inserting Plastic Pouch
11	Collecting GB	Dissector
12	Extracting Trocars	Trocars
13	Extracting Laparoscope	Laparoscope
14	Extracting GB	Scissors & Suction
15	Suturing Ports	Needles & Forceps
16	Applying a Hemostatic	Hemostatic
17	Irrigating	Irrigator
18	Stanching by Cautery	Cautery
19	Extracting Lap. for Cleaning	Extracting Laparoscope & Cleaning it with clean Gauze
20	Doing Unrelated Works	-
21	End	-

Table 1. Definitions of surgical stages in human cholecystectomy

Sequential flow of surgical stages was analyzed and a complete surgical procedure was determined and represented by a state-transition diagram as shown in figure 14. Since the surgical procedure is not deterministic procedure and has a little variance, the diagram includes the probability and the occurrence of traversing from one stage to another as shown in figures 14 and 15. In figure 15(a), white and black boxes indicate 0% and 100% probability, respectively. Figure 15(b) shows the occurrence of the transitions, and white and black boxes indicate 0 and 2.63 times/case, respectively. However, since the variance of the surgical procedure is not extreme, you can see that the probabilistic map is very sparse. In order to find out the dominant surgical stages and the dominant sequence, one or two transitions with the highest probability at each stage are chosen as shown in figure 16. The chosen transitions and the stages can be considered as the *normal surgical procedure* of human cholecystectomy.

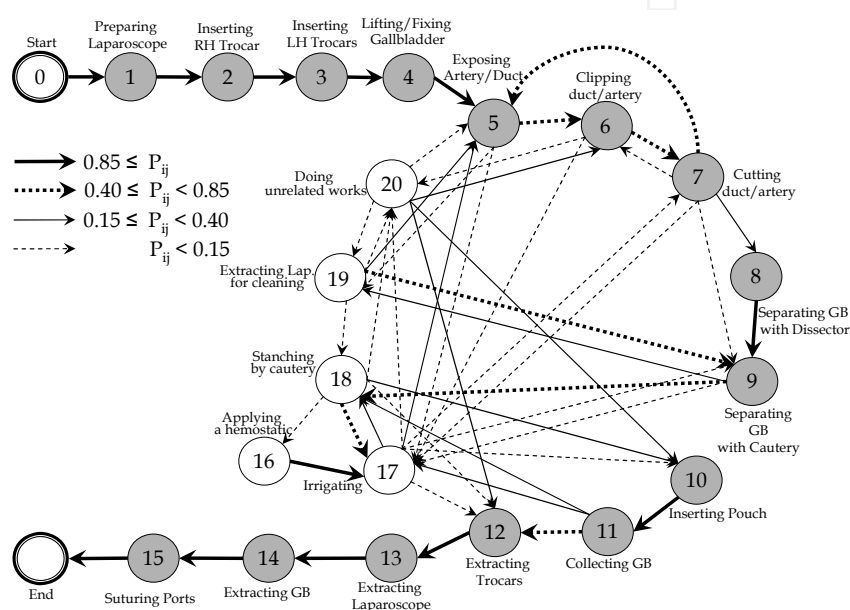
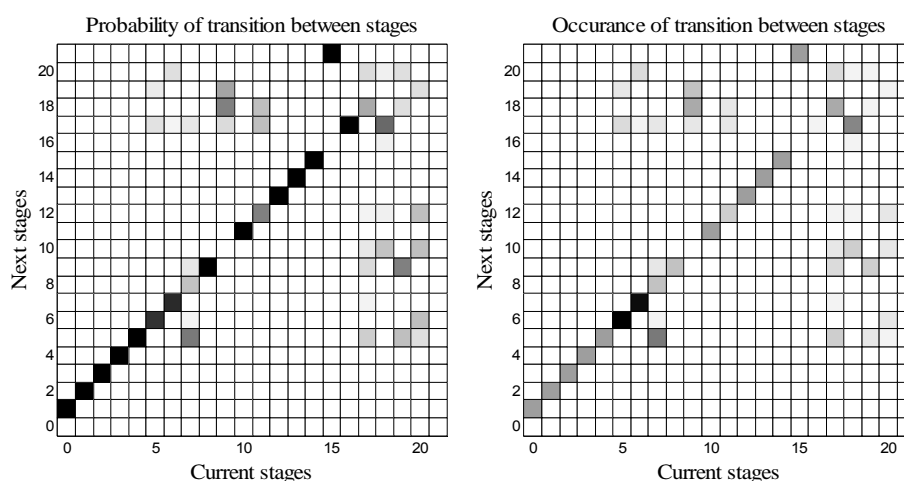


Figure 14. Surgical procedure represented in state-transition diagram with classified probability value of each transition



(a) Probability : White 0 %, Black 100% (b) Occurrence : White 0 times, Black 2.63 times

Figure 15. Probability and occurrence of transition between stages

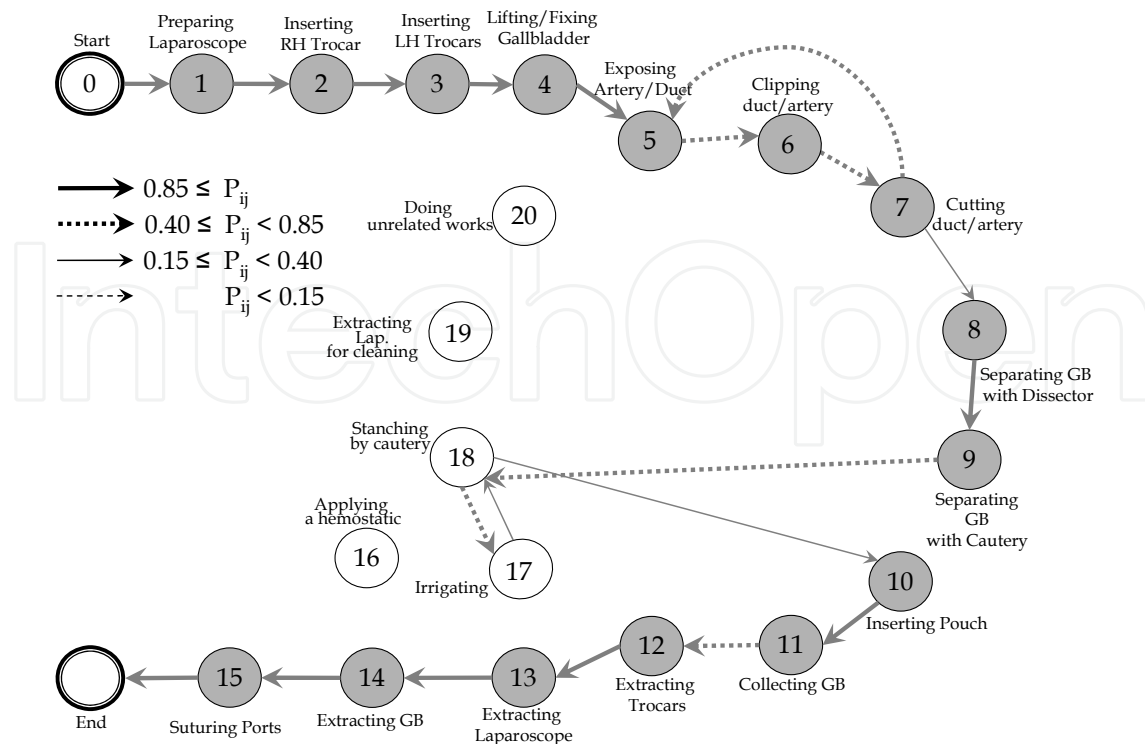


Figure 16. Normal procedure (frequent stages) in human cholecystectomy

3.4 Action Strategies: Desired Camera Viewpoint and Viewing Method

Considering that our surgery task model will be applied to a laparoscopic assistant robot, the action strategy should be related to the optimal camera view. Among the characteristics related to the camera view, the viewing method and the desired camera viewpoint at each stage were considered. To find the preferred view of the surgeon at each stage, the normal procedures of a cholecystectomy was observed through video analysis and consultation with a surgeon. These observations revealed that there are distinctive relations among the tools being utilized, tasks being performed, and the preferred camera view. At some stages, the surgeon wants the laparoscope to follow the tool tip and an assistant positions the laparoscope so that the tool tip is positioned at the center of the monitor. In some stages, the surgeon prefers the laparoscope to remain steady so as to maintain a steady view of the surgical site. The relationship among surgical stages, tools, and camera viewpoints is summarized in figure 17. This information allows us to estimate the current stage by looking at the inserted tool and the information of the previous stage.

As shown in figure 17, current stage is highly related to the tool in use. This allows us to utilize the surgical tool as a major transition condition to estimate the current surgical stage. In addition to the tool change, insertion and extraction of the laparoscope or tools are also considered as transition conditions. The only transition conditions for the normal surgical procedure are listed in table 2.

3.5 Input Information: Laparoscopic View and Surgeon's Commands

Since the type of surgical tool is a key feature for the transition condition and the tip position of the tool is important for the tool tracking capability, the laparoscopic view is determined as one of the input modalities. The method to extract the information from the laparoscopic

view is identical with the one described in section 2.4.2. The color of the middle part of the marker is also utilized to identify the inserted tool's type.

Surgical information from the laparoscopic view may not be sufficient to completely control the laparoscope throughout the surgery. Some kind of manual intervention to regulate the motion of the robot is sometimes needed. Therefore, the surgeon's voice commands are utilized to modify the view whenever the view is not satisfactory. Although the preferred camera views may have many parameters that are not explicitly represented in figure 17, i.e. tracking speed, exact location of the surgical target, the views can be generally classified as two modes: *site-keeping* mode and *tool-tracking* mode. In case of the site-keeping mode, it is

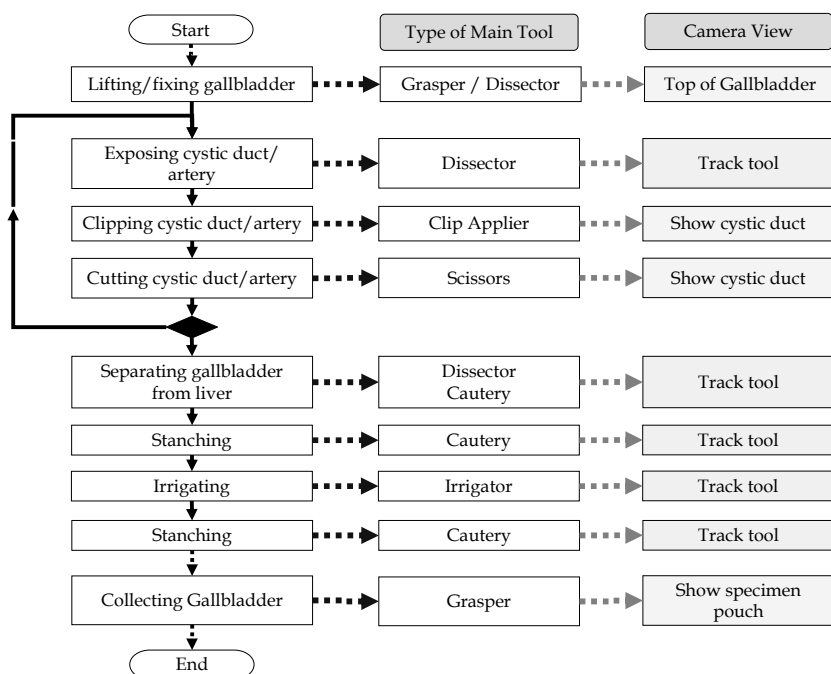


Figure 17. Relations between surgical stages, tools and camera viewpoints

Current stage	Next stage	Transition condition	Current stage	Next stage	Transition condition
0	1	Starting insertion of Lap. trocar	9	18	Finishing the separating procedure
1	2	Starting insertion of RH trocar	10	11	Inserting lap. after plastic pouch
2	3	Starting insertion of LH trocar	11	12	Starting extracting trocar
3	4	Detecting LH ratchet grasper or dissector	12	13	Starting extracting laparoscope
4	5	Detecting LH grasper	13	14	Starting extracting gallbladder
5	6	Detecting clip applier	14	15	Starting suturing ports
6	7	Detecting scissors	15	21	Finishing suturing ports
7	5	Detecting dissector	17	18	Detecting cautery
7	8	Detecting dissector	18	10	Starting extracting laparoscope
8	9	Detecting cautery	18	17	Detecting irrigator

Table 2. Transition conditions between surgical stages of the normal surgical procedure

necessary to accurately recognize the surgical site for showing the desired view. Recognition of the surgical site is left for the future works. For the time being, the desired view is determined by surgeon's voice commands. On this account, the robot's control diagram is very similar to one described in figure 10 except the viewing method is determined automatically based on the surgery task model.

3.6 Implementation and Simulation of the Surgery Task Model

To implement the surgery task model outlined in sections 3.3 to 3.5, we've composed the data in figures 15 and 16 and table 2 into a set of structured data, as shown in figure 18. The surgery task model has the total number of stages, task being performed at each stage, viewing characteristics at each stage, and a possible transition route at a given stage. The surgical tools are used as a dominant factor for estimating the transition to next stage. In this simulation, we used a normal surgical procedure shown in figure 16, rather than all procedures in general laparoscopic surgery represented by figure 14.

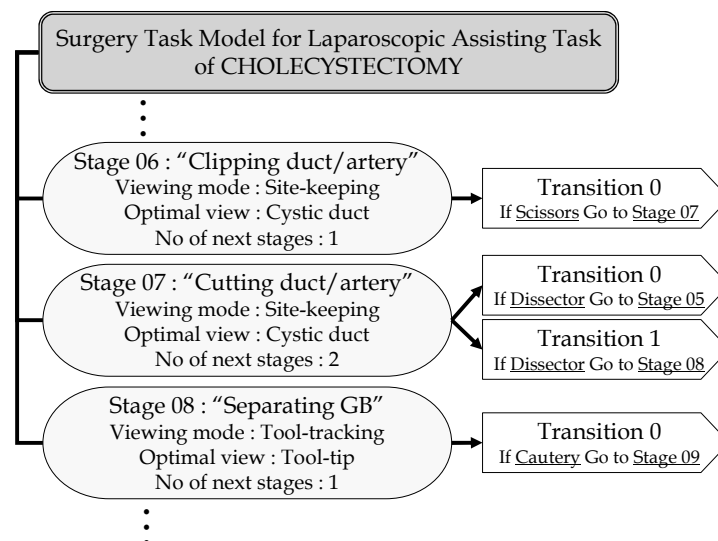


Figure 18. Data structure of surgery task model

It is possible that two or more possible next stages exist. In such case, we consider all possibilities at the given stage. In the normal cholecystectomy procedure shown in figure 16, it occurs at a "Cutting duct/artery" stage (stage 7). The next stage may be either "Separating GB with Dissector" (stage 8) or "Exposing duct/artery" (stage 5), because both the transition conditions for stages 5 and 8 are a dissector. Fortunately, the action strategies for these cases are the same, i.e. the preferred view is to "track tool," as shown in figure 17. However, since the preferred views of all possible routes at other surgeries can be different from each other, this issue should be resolved in the future work.

To verify the possibility of estimating the present stage when the state of the last stage and the type of currently inserted tool are given, a simplified simulation was performed. Since the checking mechanism related to insertion/extraction of the laparoscope and the left-hand tool is not implemented yet, this information was provided by a keystroke. The result of this simulation is shown in figure 19. Similar to the normal surgical procedure, the surgical tools are inserted into the simulated environment of the abdomen in the following order:

Dissector, Clip applicator, Scissors, Dissector, Clip applicator, Scissors, Dissector, Cautery, Irrigator, Cautery, and Dissector.

Each tool is given a unique ID (1 - Dissector, 2 - Clip applicator, 3 - Scissors, 4 - Cautery and 5 - Irrigator), as shown on the right side of figure 19(b). The identified tool type is plotted with respect to time in figure 19(b) and the estimated surgical stages during that period are plotted in figure 19(a). For example, when the clip applicator is inserted during a 36~43 sec. period (marked by ①), the estimated surgical stage can be found by tracking the symbols in figure 19(a) (“clipping duct/artery”). This prediction process uses only the information about the previous stage and the tool type, and two different stages for a given period may be expected. For example, during a 48~53 sec. period (marked by ②), the proposed interaction scheme defines the present stage as either “separating GB with Dissector” or “exposing duct/artery.” However, since the next instrument is identified as the clip applicator, the next stage can be estimated as the “clipping duct/artery” stage (stage 6).

The prediction process is conducted only when the tools are identifiable. When the tool is not detected or identified, the scheme does not change the current stage. At the beginning and end of the surgery, where no tool-stage relationship is defined, a time sequence is used to represent the preparation (stages 0~3) and wrap-up procedures (stages 12~15 and 21).

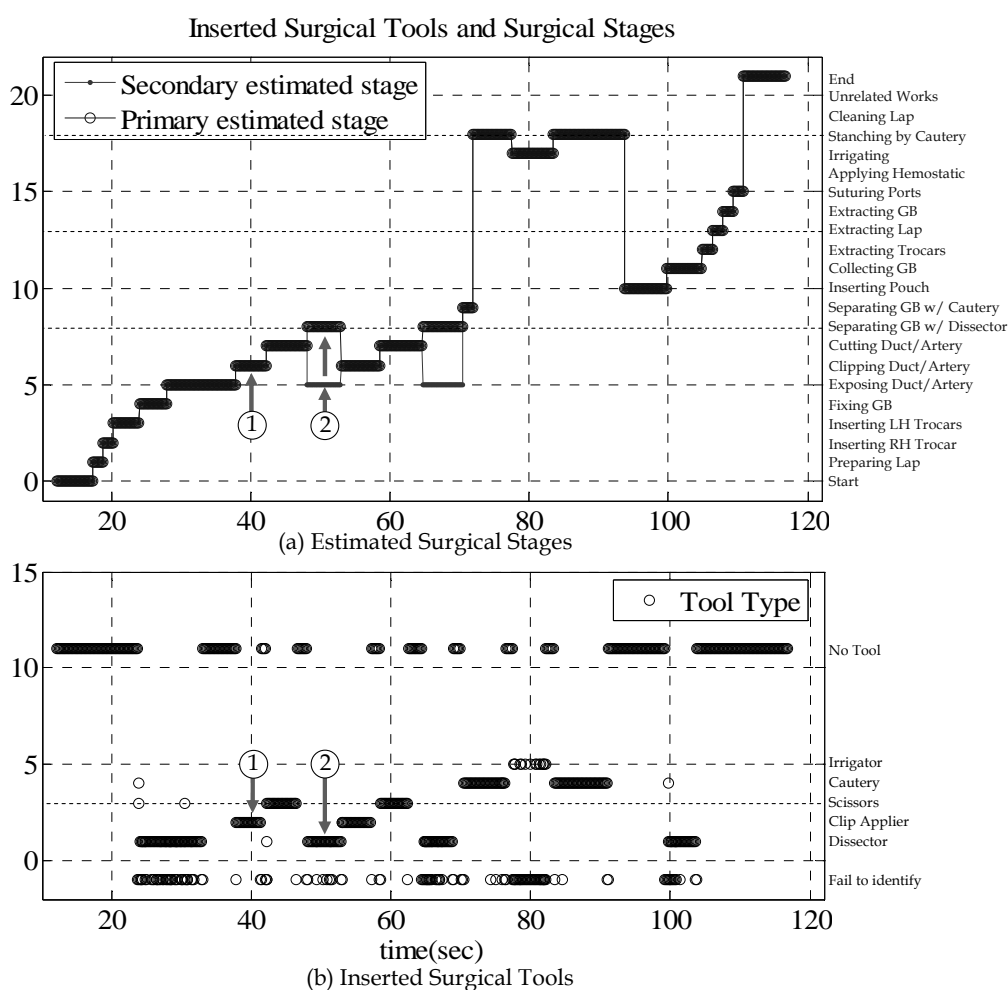
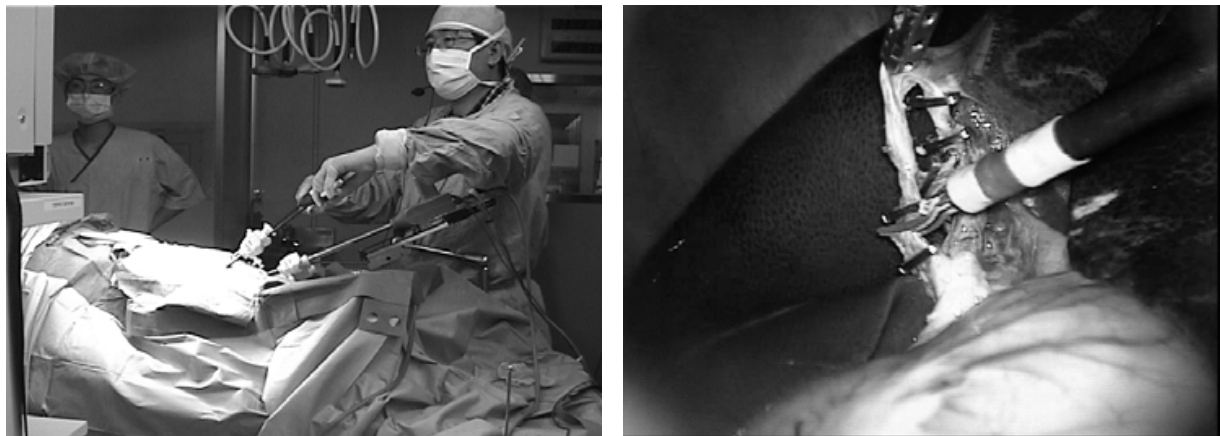


Figure 19. Implemented interaction based on the proposed surgery task model

4. In Vivo Experiments

4.1 Verification of Mechanical Properties

Three cases of porcine cholecystectomy were performed to evaluate the performance of KaLAR. The objective of these trials are: (a) to determine if the workspace covered by the robot is sufficient for cholecystectomy, (b) to see if solo-surgery is possible with the proposed control scheme, and (c) the time required to complete the surgery is comparable to other robot-assisted and human-assisted cholecystectomy. The materials used were three female pigs of 3~4 months old and weigh approximately 30 kg. The size of their abdominal cavity was smaller than that of an adult person and thus, the trocar for laparoscope had to be placed below the navel. Since the KaLAR's initial position influences the motion range, it is necessary to place it carefully during the initialization procedure. The cholecystectomy mainly deals with the gallbladder located beneath the liver. Thus, KaLAR's position was adjusted with a passive holder so that it shows the lower part of the liver. All three surgeries were performed by one surgeon as shown in figure 20 and all the surgical procedures were in accordance with the guidelines enforced by the local ethics committees.



(a) Solo-surgery

(b) Internal View

Figure 20. Porcine cholecystectomy with KaLAR

Through animal tests, we were able to confirm that the workspace covered by KaLAR is sufficient for porcine cholecystectomy and the control of the robot using voice commands and visual-servoing is effective enough for solo-surgery. The surgical time comparison with other robot-assisted and human-assisted porcine cholecystectomies is summarized in Table 3, where the surgical time was defined as the time between initial insertion and final extraction of KALAR. The surgical times described in the work by Kobayashi et al. were recalculated in terms of our definition, that is, we have subtracted the trocar insertion time from the total operating time (Kobayashi et al., 1999). Although we only have a limited number of surgeries and the time measurement can only be used for a rough estimate of the robot's performance, the time spent for porcine cholecystectomy can be said to be comparable to other robot-assisted and human-assisted porcine cholecystectomy. Note that the time difference for between experiments with KaLAR and the other system seems to be mainly caused by the surgeon's expertise level, considering our surgeon's operating time (23.3 ± 9.9 minutes for four cases) for the human cholecystectomy with a conventional rigid scope is slightly shorter than for these experiments using KaLAR.

Target and material	Time (min)
On a pig with Kobayashi's system (Kobayashi et al., 1999)	38 (one case)
On a pig with a human assistant (Kobayashi et al., 1999)	41.6 (ten cases)
On a pig with the KaLAR system	26.7±8.3 (three cases)

Table 3. Surgical time for porcine cholecystectomy

4.2 Preliminary Experiment with Surgery Task Model

This section will describe the results of the *in vivo* tests from the perspective of the proposed interaction scheme. For this purpose, the second and third experiments were analyzed and compared because they were performed with different interaction schemes. In the third experiment (Exp. A), the surgeon arbitrarily determined the control mode at different stages of surgery by issuing "tracking mode" or "voice mode" command. In the second experiment (Exp. B), simplified version of the proposed interaction method was implemented and the surgeon had no control over the control mode. In this test, only the normal surgical procedure was considered and the camera view was selected mainly based on the tool-viewpoint relation shown in figure 17. We measured the surgical time and the number of voice commands issued during each surgery. Table 4 indicates that the surgical time was increased but the number of voice commands was reduced with the proposed scheme. In Table 4, the number of issued voice commands is counted excluding the commands during preparation stages. While the results do not provide conclusive evidence of the efficacy of the proposed scheme, it may be worthwhile to conduct more experiments to see if the proposed scheme can reduce the number of commands and thus, less control burden.

	Operating Time (min.)	No. of Voice Commands
<i>In vivo</i> experiment with surgeon's ability to decide viewing mode (Exp. A)	20	71
<i>In vivo</i> experiment with the proposed interaction scheme (Exp. B)	24	50

* The operating time and the number of voice commands are measured excluding the results during the preparation procedure.

Table 4. Results of *in vivo* porcine cholecystectomy

5. Conclusion and Discussion

To develop an intelligent laparoscopic assistant robot, the mechanism should be designed so that the robotic system can be easily handled in real operation environment, and to give *task-specific* intelligence to medical robot, the robotic system should have well-structured task model of the surgery. On these grounds, this chapter describes the intelligent laparoscopic assistant robot, KaLAR, focusing on (a) its compactness and convenience, and (b) its novel interaction scheme through a surgery task model. Unlike previous robotic systems, the robot uses an internally bending mechanism and constrains the motions within the abdomen. This approach is expected to reduce the potential risk of interfering with surgical staff. The inherent hysteresis characteristics of the mechanism were compensated for more accurate control. In order to facilitate easy operation, a voice interface and a visual-servoing method were introduced and implemented. To verify the applicability of KaLAR, three

solo-surgeries on porcine cholecystectomy were performed. These *in vivo* animal tests show that the mechanical structure of the KaLAR system is acceptable in the surgical environment and has sufficient workspace to provide necessary views during cholecystectomy.

In order to implement a task-specific intelligence for assistant robot, we proposed a surgery task model, which includes the surgical procedure (sequence of surgical stages), input information on the surgical environment, and actions strategies composed of proper viewing mode and viewpoint at each stage. We believe that the surgery task model makes it possible to realize ideal surgeon-robot interaction. In this model, the surgical procedure is extracted through a video analysis and represented as a state-transition diagram. For input information, the laparoscopic view and the operating surgeon's voice commands are utilized. To verify the possibility to realize the interaction scheme based on the surgery task model and to assess the effectiveness of the scheme, the model was integrated to the KaLAR system. Although the issued voice commands were not remarkably reduced, the surgery task model's applicability in real surgery is demonstrated through an *in vivo* porcine cholecystectomy. Although statistically insufficient, the results of our preliminary experiments show that the proposed interaction has the potential to reduce the surgeon's control burden and allow the surgeon to control the robot naturally.

Despite KaLAR's applicability, several issues should be solved. In case of the mechanical issues, the length of the bending tip should be shortened because its lengthiness can restrict the reachable area. There is the potential harmfulness caused by the robot's malfunction, especially during the zooming motion. To reduce the possibility of the malfunction, we will introduce the additional sensor to confirm the actuators' position measured in the zooming motion. Next, for the issues related to the interaction scheme, the optimal view in the site-keeping mode needs to be determined in a more systematic manner and an identification method for insertion/extraction of the laparoscope and the left-hand tools are required to make the proposed scheme more effective. In dealing with the variance in surgery, a method to utilize the whole model described in figure 14 should be considered. Also, the possibility of misidentification of the transition condition and the robustness of the surgical procedure should be investigated. Finally, more *in vivo* tests are required for more quantitative evaluation and for its extensibility to other minimally invasive surgeries

6. References

- Allaf, M. E.; Jackman, S. V.; Schulam, P. G.; Cadeddu, J. A.; Lee, B. R.; Moore, R. G. & Kavoussi, L. R. (1998). Laparoscopic visual field : Voice vs foot pedal interfaces for control of the AESOP robot, *Surgical Endoscopy*, Vol.12, (pp. 1415-1418), 0930-2794
- Berkelman, P.; Cinquin, P.; Troccaz, J.; Ayoubi, J.; Letoublon, C. & Bouchard, F. (2002). A Compact, Compliant Laparoscopic Endoscope Manipulator, *Proceedings of IEEE International Conference on Robotics & Automation*, pp. 1870-1875, 0-7803-7272-7, Washington, DC, May, 2002
- Casals, A.; Amat, J. & Laporte, E. (1996). Automatic Guidance of an Assistant Robot in Laparoscopic Surgery, *Proceedings of the IEEE International Conference on Robotics and Automation*, pp. 895-900, 0-7803-2988-4, Minneapolis, Minnesota, April, 1996

- Cassandras, C. G. & Lafortune, S. (1999). *Introduction to Discrete Event Systems*, Kluwer Academic Publishers, 0-7923-8609-4, Norwell, MAÇavuşoğlu, M. C.; Villanueva, I. & Tendick, F. (2001). Workspace Analysis of Robotic Manipulators for a Teleoperated Suturing Task, *Proceedings of the IEEE/RSJ International Conference on Intelligent Robots and Systems*, pp. 2234-2239, 0-7803-6612-3, Maui, HI, October - November, 2001
- Finlay, P. A. (1996). Clinical experience with a goniometric head-controlled laparoscope manipulator, *Proceedings of IARP Workshop on Medical Robotics*, Vienna, Austria
- Franzino, R. J. (2003). The Laprotek surgical system and the next generation of robotics, *Surgical Clinics of North America*, Vol.83, (pp. 1317-1320), 0039-6109
- Ghodoussi, M.; Butner, S. E. & Wang, Y. (2002). Robotic Surgery - The Transatlantic Case, *Proceedings of IEEE International Conference on Robotics & Automation*, pp. 1882-1888, 0-7803-7272-7, Washington, DC, May, 2002
- Guthart, G. S. & Salisbury, J. K. (2000). The Intuitive™ Telesurgery System: Overview and Application, *Proceedings of IEEE International Conference on Robotics & Automation*, pp. 618-621, 0-7803-5886-4, San Francisco, CA, April, 2000
- Ikuta, K.; Hasegawa, T. & Daifu, S. (2003). Hyper Redundant Miniature Manipulator "Hyper Finger" for Remote Minimally Invasive Surgery in Deep Area, *Proceedings of IEEE International Conference on Robotics & Automation*, pp. 1098-1102, 0-7803-7736-2, Taipei, Taiwan, September, 2003
- Johnson, P. (1992). *Human-Computer Interaction: Psychology, Task Analysis and Software Engineering*, McGRAW-HILL Book Company Europe, 0077072359, UK
- Kim, J.; Lee, Y.-J.; Ko, S.-Y.; Kwon, D.-S. & Lee, W.-J. (2004). Compact Camera Assistant Robot for Minimally Invasive Surgery: KaLAR, *Proceedings of IEEE/RSJ International Conference on Intelligent Robots and Systems*, pp. 2587-2592, 0-7803-8463-6, Sendai, Japan, Sept.-Oct., 2004
- Ko, S.-Y.; Kim, J.; Lee, W.-J. & Kwon, D.-S. (2007a). Compact laparoscopic assistant robot using a bending mechanism, *Advanced Robotics*, Vol.21, No.5-6, (pp. 689-709), 0169-1864
- Ko, S.-Y.; Kim, J.; Lee, W.-J. & Kwon, D.-S. (2007b). Surgery Task Model for Intelligent Interaction between Surgeon and Laparoscopic Assistant Robot, *International Journal of Assistive Robotics and Mechatronics* Vol.8, No.1, (pp. 38-46), 1975-0153
- Kobayashi, E.; Masamune, K.; Sakuma, I.; Dohi, T. & Hashimoto, D. (1999). A New Safe Laparoscopic Manipulator System with a Five-Bar Linkage Mechanism and an Optical Zoom, *Computer Aided Surgery*, Vol.4, No.4, (pp. 182-192), 1092-9088
- Lee, K.; Kim, H.-R.; Yoon, W. C.; Yoon, Y.-S. & Kwon, D.-S. (2005). Designing a human-robot interaction framework for home service robot, *Proceedings of IEEE International Workshop on Robot and Human Interactive Communication*, pp. 286-293, 0-7803-9275-2, Nashville, TN, August, 2005
- Lee, Y.-J. (2004). Development of a Compact Laparoscopic Assistant Robot: KaLAR, *Master's thesis*, Korea Advanced Institute of Science and Technology, Daejeon Korea
- MacKenzie, C. L.; Ibbotson, J. A.; Cao, C. G. L. & Lomax, A. J. (2001). Hierarchical decomposition of laparoscopic surgery : a human factors approach to investigating the operating room environment, *Minimally Invasive Therapy and Allied Technologies*, Vol.10, No.3, (pp. 121-127), 1364-5706

- Mitsuishi, M.; Arata, J.; Tanaka, K.; Miyamoto, M.; Yoshidome, T.; Iwata, S.; Warisawa, S. & Hashizume, M. (2003). Development of a Remote Minimally-Invasive Surgical System with Operational Environment Transmission Capability, *Proceedings of IEEE International Conference on Robotics & Automation*, pp. 2663-2670, 0-7803-7736-2, Taipei, Taiwan, September, 2003
- Nishikawa, A.; Asano, S.; Fujita, R.; Yohda, T.; Miyazaki, F.; Sekimoto, M.; Yasui, M.; Takiguchi, S. & Monden, M. (2003). Robust Visual Tracking of Multiple Surgical Instruments for Laparoscopic Surgery, *Proceedings of Computer Assisted Radiology and Surgery*, London, UK
- Nishikawa, A.; Hosoi, T.; Koara, K.; Negoro, D.; Hikita, A.; Asano, S.; Miyazaki, F.; Sekimoto, M.; Miyake, Y.; Yasui, M. & Monden, M. (2001). Real-Time Visual Tracking of the Surgeon's Face for Laparoscopic Surgery, *Lecture Notes in Computer Science*, Vol.2208, (pp. 9-16), 0302-9743
- Ohnuma, K.; Masamune, K.; Yoshimitsu, K.; Shinohara, K.; Vain, J.; Fukui, Y. & Miyawaki, F. (2005). Surgical Scenario for Lapsaroscopic Surgery with Timed Automata and Development of Scrub Nurse Robot - Application of Human Adaptive Mechatronics to surgical support system, *Proceedings of the 2nd COE workshop on Human Adaptive Mechatronics(HAM)*, pp. 163-166, Japan, March, 2005
- Riener, R.; Reiter, S.; Rasmus, M.; Wetzel, D. & Feussner, H. (2003). Acquisition of arm and instrument movements during laparoscopic interventions, *Minimally Invasive Therapy & Allied Technologies*, Vol.12, No.5, (pp. 235-240), 1364-5706
- Rosen, J.; Brown, J. D.; Chang, L.; Sinanan, M. N. & Hannaford, B. (2006). Generalized Approach for Modeling Minimally Invasive Surgery as a Stochastic Process Using a Discrete Markov Model, *IEEE Transactions on Biomedical Engineering*, Vol.53, No.3, (pp. 399-413), 0018-9294
- Simaan, N.; Taylor, R. & Flint, P. (2004). High Dexterity Snake-Like Robotic Slaves for Minimally Invasive Telesurgery of the Upper Airway, *Lecture Notes in Computer Science*, Vol.3217, (pp. 17-24), 0302-9743
- Tanaka, H. (1978). Articulated, Four-way Bendable Tube Structure, US Patent 4108211
- Taylor, R. H.; Funda, J.; Eldridge, B.; Gomory, S.; Gruben, K.; LaRose, D.; Talamini, M.; Kavoussi, L. & Anderson, J. (1995). A Telerobotic Assistant for Laparoscopic Surgery, *IEEE Engineering in Medicine and Biology*, Vol.14, No.3, (pp. 279-288), 0739-5175
- Wang, Y.-F.; Uecker, D. R. & Wang, Y. (1996). Choreographed Scope Maneuvering in Robotically-Assisted Laparoscopy with Active Vision Guidance, *Proceedings of IEEE Workshop on Applications of Computer Vision*, pp. 187-192, 0-8186-7620-5, Sarasota, FL, December, 1996
- Wei, G.-Q.; Arbter, K. & Hirzinger, G. (1997). Real-Time Visual Servoing for Laparoscopic Surgery : Controlling Robot Motion with Color Image Segmentation, *IEEE Engineering in Medicine and Biology*, Vol.16, No.1, (pp. 40-45), 0739-5175
- Yamashita, H.; Kim, D.; Hata, N. & Dohi, T. (2003). Multi-Slider Linkage Mechanism for Endoscopic Forceps Manipulator, *Proceedings of the IEEE/RSJ International Conference on Intelligent Robots and Systems*, pp. 2577-2582, 0-7803-7860-1, Las Vegas, Nevada, October, 2003
- Yoon, W. C. (2005). Cognitive Human-Robot Interaction: Groping for Dialogue Intelligence, *Robot and Human : Korea Robotics Society Review*, Vol.2, No.3, (pp. 29-43), 1738-4796, (Written in Korean)



Medical Robotics

Edited by Vanja Bozovic

ISBN 978-3-902613-18-9

Hard cover, 526 pages

Publisher I-Tech Education and Publishing

Published online 01, January, 2008

Published in print edition January, 2008

The first generation of surgical robots are already being installed in a number of operating rooms around the world. Robotics is being introduced to medicine because it allows for unprecedented control and precision of surgical instruments in minimally invasive procedures. So far, robots have been used to position an endoscope, perform gallbladder surgery and correct gastroesophageal reflux and heartburn. The ultimate goal of the robotic surgery field is to design a robot that can be used to perform closed-chest, beating-heart surgery. The use of robotics in surgery will expand over the next decades without any doubt. Minimally Invasive Surgery (MIS) is a revolutionary approach in surgery. In MIS, the operation is performed with instruments and viewing equipment inserted into the body through small incisions created by the surgeon, in contrast to open surgery with large incisions. This minimizes surgical trauma and damage to healthy tissue, resulting in shorter patient recovery time. The aim of this book is to provide an overview of the state-of-art, to present new ideas, original results and practical experiences in this expanding area. Nevertheless, many chapters in the book concern advanced research on this growing area. The book provides critical analysis of clinical trials, assessment of the benefits and risks of the application of these technologies. This book is certainly a small sample of the research activity on Medical Robotics going on around the globe as you read it, but it surely covers a good deal of what has been done in the field recently, and as such it works as a valuable source for researchers interested in the involved subjects, whether they are currently “medical roboticists” or not.

How to reference

In order to correctly reference this scholarly work, feel free to copy and paste the following:

Dong-Soo Kwon, Seong-Young Ko and Jonathan Kim (2008). Intelligent Laparoscopic Assistant Robot through Surgery Task Model: How to Give Intelligence to Medical Robots, Medical Robotics, Vanja Bozovic (Ed.), ISBN: 978-3-902613-18-9, InTech, Available from:

http://www.intechopen.com/books/medical_robotics/intelligent_laparoscopic_assistant_robot_through_surgery_task_model__how_to_give_intelligence_to_med

INTECH
open science | open minds

InTech Europe

University Campus STeP Ri
Slavka Krautzeka 83/A

InTech China

Unit 405, Office Block, Hotel Equatorial Shanghai
No.65, Yan An Road (West), Shanghai, 200040, China

51000 Rijeka, Croatia
Phone: +385 (51) 770 447
Fax: +385 (51) 686 166
www.intechopen.com

中国上海市延安西路65号上海国际贵都大饭店办公楼405单元
Phone: +86-21-62489820
Fax: +86-21-62489821

IntechOpen

IntechOpen

© 2008 The Author(s). Licensee IntechOpen. This chapter is distributed under the terms of the [Creative Commons Attribution-NonCommercial-ShareAlike-3.0 License](#), which permits use, distribution and reproduction for non-commercial purposes, provided the original is properly cited and derivative works building on this content are distributed under the same license.

IntechOpen

IntechOpen